Lawrence Berkeley National Laboratory

Lawrence Berkeley National Laboratory

Title

Enhanced geothermal systems (EGS) using CO2 as working fluid - A novelapproach for generating renewable energy with simultaneous sequestration of carbon

Permalink

https://escholarship.org/uc/item/9ww907cb

Author

Pruess, Karsten

Publication Date

2006-06-07

Peer reviewed

Enhanced Geothermal Systems (EGS) Using CO₂ as Working Fluid – A Novel Approach for Generating Renewable Energy with Simultaneous Sequestration of Carbon

Karsten Pruess

Earth Sciences Division, Lawrence Berkeley National Laboratory
Berkeley, CA 94720

K_Pruess@lbl.gov

Abstract

Responding to the need to reduce atmospheric emissions of carbon dioxide, Donald Brown (2000) proposed a novel enhanced geothermal systems (EGS) concept that would use CO_2 instead of water as heat transmission fluid, and would achieve geologic sequestration of CO_2 as an ancillary benefit. Following up on his suggestion, we have evaluated thermophysical properties and performed numerical simulations to explore the fluid dynamics and heat transfer issues in an engineered geothermal reservoir that would be operated with CO_2. We find that CO_2 is superior to water in its ability to mine heat from hot fractured rock. CO_2 also has certain advantages with respect to wellbore hydraulics, where larger compressibility and expansivity as compared to water would increase buoyancy forces and would reduce the parasitic power consumption of the fluid circulation system. While the thermal and hydraulic aspects of a CO_2-EGS system look promising, major uncertainties remain with regard to chemical interactions between fluids and rocks. An EGS system running on CO_2 has sufficiently attractive features to warrant further investigation.

INTRODUCTION

The resource base for geothermal energy is enormous, but commercial production of geothermal energy is currently limited to hydrothermal systems, in which naturally present fracture networks permit fluid circulation, and allow geothermal heat to be produced by tapping these hot fluids through wellbores. Most geothermal resources occur in rocks that lack fracture permeability and fluid circulation. The "enhanced" or "engineered" geothermal systems concept (EGS) aims to extract geothermal energy from these resources by (1) creating permeability through hydraulic stimulation or fracturing, which involves fluid injection through deep boreholes to activate existing rock fractures or create new ones, and (2) setting up and maintaining fluid circulation through these fracture networks by means of a system of injection and production boreholes, so that the thermal energy can be transmitted to the land surface for human use.

Previous attempts to develop EGS in the U.S., Japan, Europe and Australia have all employed water as a heat transmission fluid. Water has many properties that make it a favorable medium for this purpose, but it also has serious drawbacks. An unfavorable property of water is that it is a powerful solvent for many rock minerals, especially at elevated temperatures. Injecting water into hot rock fractures causes strong dissolution and precipitation effects that change fracture permeability and make it very difficult to operate an EGS reservoir in a stable manner (Xu and Pruess, 2004). Also, water is a sparse and valuable commodity in many areas, as e.g. the western U.S., and inevitable water losses during fluid circulation can be a severe economic liability.

Responding to the need to reduce atmospheric emissions of carbon dioxide, Donald Brown (2000) proposed a novel EGS concept that would use CO_2 instead of water as heat transmission fluid, and would achieve geologic storage of CO_2 as an ancillary benefit. Brown noted that CO_2 has certain physical and chemical properties that would be favorable for operation of an EGS system. Favorable properties of CO_2 emphasized by Brown include the following:

- large expansivity would generate large density differences between the cold CO_2 in the injection well and the hot CO_2 in the production well, and would provide buoyancy force that would reduce the power consumption of the fluid circulation system;
- lower viscosity would yield larger flow velocities for a given pressure gradient; and

- CO_2 would be much less effective as a solvent for rock minerals, which would reduce or eliminate scaling problems, such as silica dissolution and precipitation in water-based systems.

Brown also noted the lower mass heat capacity of CO_2 as an unfavorable property, but pointed out that this would be partially compensated by the greater flow capacity of CO_2 due to lower viscosity. Fouillac et al. (2004) suggested that an EGS using CO_2 as heat transmission fluid could have favorable geochemical properties, as CO_2 uptake and sequestration by rock minerals would be quite rapid. A preliminary evaluation of CO_2 as a working fluid for EGS was presented by Pruess and Azaroual (2006). Their findings suggest that CO_2 is roughly comparable to water as a heat transmission fluid, while offering distinct advantages for wellbore hydraulics.

The present paper compares thermophysical properties of CO_2 and water, and examines pressure and temperature conditions for flow of CO_2 in wellbores as well as in reservoirs with predominant fracture permeability. Comparisons are made with the flow behavior of water, in order to identify favorable as well as unfavorable characteristics of CO_2 as an EGS working fluid. We also present preliminary considerations on chemical aspects of a CO_2-EGS system.

THERMOPHYSICAL PROPERTIES

Fig. 1 shows the phase diagram for CO_2 in the range of temperature and pressure conditions that are of interest for injection into and production from enhanced geothermal systems. The critical point of CO_2 is at $T_{crit} = 31.04$ °C, $P_{crit} = 73.82$ bar (Vargaftik, 1975). At lower (subcritical) temperatures and/or pressures, CO_2 can exist in two different phases, a liquid and a gaseous state, as well as two-phase mixtures of these states (Fig. 1). Supercritical CO_2 forms a phase that is distinct from the aqueous phase and can change continuously into either gaseous or liquid CO_2 with no phase boundaries.
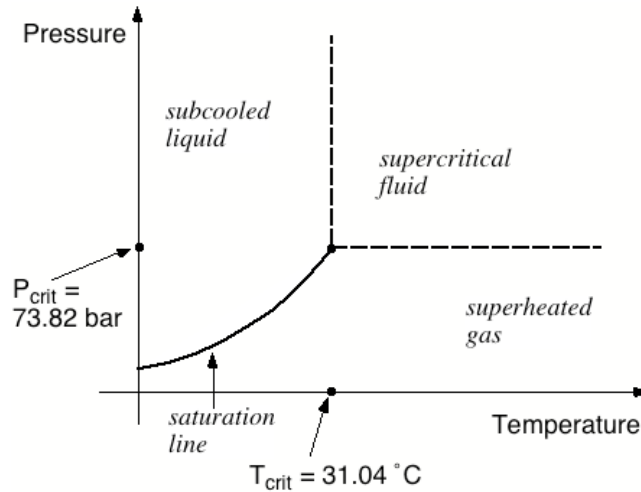
Figure 1. Phase states of CO_2.

Fluid mass flow rates for a given driving force are proportional to the ratio of density to viscosity, $m = \rho/\mu$. The sensible heat carried by mass flow is proportional to the specific enthalpy of the fluid. Additional parameters that are important for mass flow and heat transfer behavior include compressibility $c = (1/\rho)(\partial\rho/\partial P)$ and thermal expansivity $\varepsilon = -(1/\rho)(\partial\rho/\partial T)$.

Figs. 2 and 3 present thermophysical properties of CO_2 and water. CO_2 properties were calculated from the correlations of Altunin (Altunin, 1975; Pruess and García, 2002). We began using Altunin's correlations in 1999 when a computer program implementing them was conveniently made available to us by Victor Malkovsky of the Institute of Geology of Ore Deposits, Petrography, Mineralogy and Geochemistry (IGEM) of the Russian Academy of Sciences, Moscow. Altunin's correlations were subsequently extensively cross-checked against experimental data and alternative PVT formulations, such as Span and Wagner (1996), and were found to be very accurate (García, 2003). Water properties were obtained from the steam table equations as given by the International Formulation Committee (IFC, 1967).

The ratio of density to viscosity is generally larger for CO_2 than for water, and dependence on temperature and pressure conditions is very different for the two fluids (Fig. 2). For water this ratio is mostly a function of temperature, with only weak dependence on pressure, reflecting the

primary dependence of both water density and viscosity on temperature. For CO_2, density and viscosity have significant dependence on both temperature and pressure. The variations are such that (ρ/μ) attains maximum values in a region that is emanating from the CO_2 saturation line, becoming smaller for liquid-like CO_2 (low T, high P) and for gas-like CO_2 (high T, low P). For (T, P)- conditions relevant for fluid injection, $T \leq 50\ ^\circ C$, (ρ/μ) for CO_2 is larger than for water by factors of 4-10. For temperatures near 200 °C, (ρ/μ) for CO_2 is larger than for water by approximately a factor 2 at high pressures, while at pressures below 150 bar, water has the larger (ρ/μ).

Fig. 3 compares the specific enthalpies for CO_2 and water. In both cases the reference state (zero enthalpy) was chosen as (T, P) = (20 °C, 100 bar). At high pressures near 500 bar, the increase of specific enthalpy with temperature for CO_2 is less than half of the increase for water, indicating that more than twice the CO_2 mass flow rate would be needed to achieve the same rate of sensible heat transport. Specific enthalpy of liquid water depends primarily on temperature, with only a weak pressure dependence. For CO_2 the pressure dependence is weak for liquid-like conditions, but becomes increasingly strong at lower pressures and higher temperatures. For adiabatic (thermally insulated) decompression, thermodynamic conditions will move along isenthalps (lines of constant specific enthalpy). Accordingly, decompression of hot, high-pressure CO_2 will be accompanied by substantial temperature decline, while for liquid water there would be a small temperature increase.

Table 1 shows that CO_2 is substantially more compressible than water, and has larger expansivity as well, especially at lower temperatures. Fluid densities will therefore vary much more strongly for CO_2 than for water as functions of pressure and temperature changes.
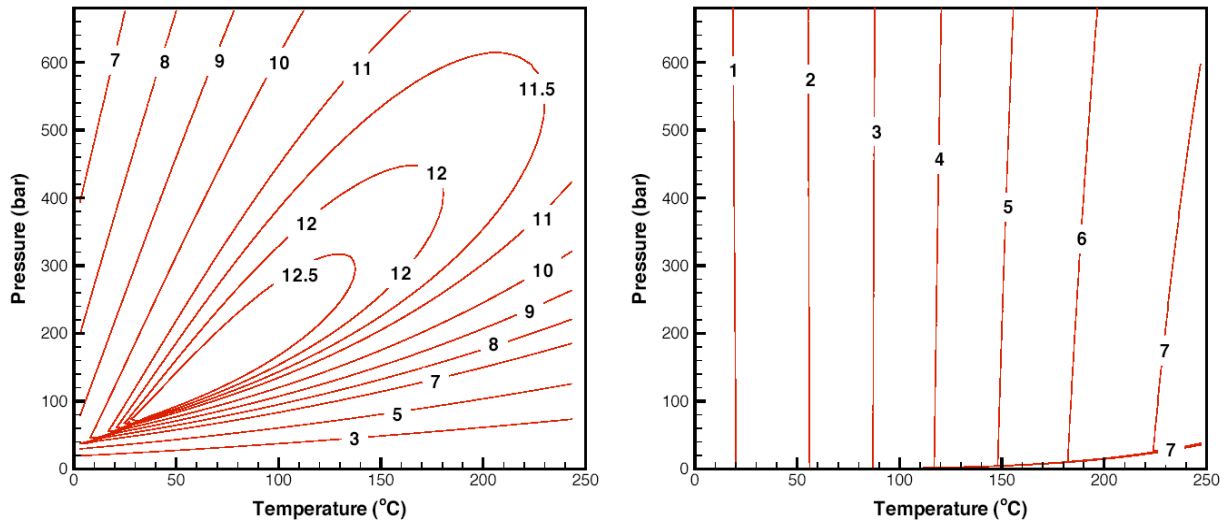
Figure 2. Ratio of fluid density to viscosity in units of 10^6 sm^{-2} for CO_2 (left) and water (right).
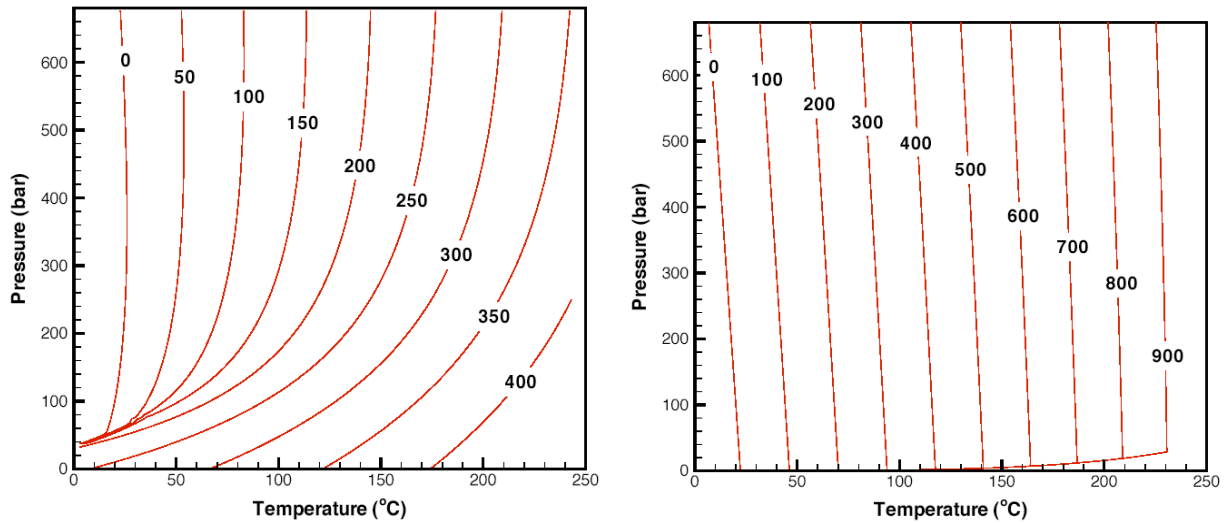

Figure 3. Specific enthalpy of CO_2 (left) and water (right) in units of kJ/kg, as function of temperature and pressure.

Table 1. Density, compressibility, and expansivity of CO_2 and water at selected (T, P)-conditions.

T (°C)	P (bar)	CO_2			water		
		ρ (kg/m^3)	compress-ibility (1/Pa)	expansivity (1/°C)	ρ (kg/m^3)	compress-ibility (1/Pa)	expansivity (1/°C)
20	100	856.251	1.490e-8	8.607e-3	1001.76	3.489e-10	1.944e-4
	500	1048.77	2.484e-9	2.696e-3	1015.94	3.538e-10	1.448e-4
200	100	122.184	1.076e-7	3.036e-3	870.798	8.377e-10	1.321e-3
	500	581.322	1.274e-8	3.172e-3	900.990	8.668e-10	1.077e-3

WELLBORE FLOW

The pressure gradient in a flowing well can be represented by a superposition of gravity, frictional, and acceleration terms (Brill and Mukherjee, 1999),

$$\nabla P = (\nabla P)_{grav} + (\nabla P)_{fric} + (\nabla P)_{acc} \qquad (1)$$

For most applications of interest, the gravitational contribution to the pressure gradient is by far the dominant term, with frictional and inertial pressure gradients contributing typically a few percent or less. In a first effort to evaluate the pressures in EGS injection and production wells, we consider only the dominant gravitational gradient.

In an injection well, temperatures will increase with depth, primarily because of heat transfer from the surrounding rocks (Ramey, 1962). Additional temperature changes are expected as a consequence of fluid compression due to pressure increase. The latter effect is very small for water, but could be more significant for the highly compressible CO_2. Similarly, in a production well the temperature of a fluid parcel flowing upward will decrease due to heat loss to the surrounding formations. Additional temperature change will occur from decompression, which is expected to be a small effect for water, but could be significant for CO_2.

The temperature effects from heat exchange with the surroundings are of a transient nature and will diminish over time. In order to obtain a basic comparison between the pressure behavior of water and CO_2 wells, we start from the simplest possible approximation to temperature conditions: we consider an injection well that is entirely at the injection (wellhead) temperature T_{inj}, and a production well that is entirely at the production (downhole) temperature T_{pro}. In order to calculate the static pressure profile in a well, the well depth z is divided into N increments, $\Delta z = z/N$. The calculation proceeds recursively from level $n\Delta z$ to $(n+1)\Delta z$ by assigning $P_{n+1} = P_n + \rho_n g \Delta z$, where $\rho_n = \rho(T_n, P_n)$, and $g = 9.81$ m^2/s is gravitational acceleration. For definiteness, we adopt parameters applicable to the European EGS experiment at Soultz, and take a well depth of 5,000 m, with a downhole temperature of $T_{pro} = 200$ ˚C (Baria et al., 2005; Dezayes et al., 2005). Injection temperature is set at $T_{inj} = 20$ ˚C.

For both water and CO_2 we start from an injection wellhead pressure of 57.4 bar, slightly in excess of the CO_2 saturation pressure at injection temperature ($P_{sat,CO2} = 57.36$ bar at $T_{inj} = 20$ ˚C). Corresponding static downhole pressures at 5,000 m depth are 528.7 bar for CO_2 and 553.4 bar for water (Fig. 4). Using these downhole pressures as starting values, we then obtain static pressures in the production well by integrating upwards at T = 200 ˚C. This results in production wellhead pressures of 288.1 bar for CO_2 and 118.6 bar for water. The difference in wellhead pressures between production and injection wells is 230.7 bar for CO_2 and 61.2 bar for water, indicating that a CO_2 circulation system would have far stronger buoyant drive, and would require less power to operate.

A more realistic outlook on longer-term P,T-conditions in flowing injection and production wells can be obtained by approximating fluid flow in the wellbore as isenthalpic. This approximation is often referred to as "adiabatic;" it ignores heat transfer between the wellbore fluid and the surroundings, which is appropriate for longer-term flow behavior. The isenthalpic flow approximation accounts for temperature changes that arise from (de-)compression of fluids, the so-called Joule-Thomson effect (Katz and Lee, 1990).
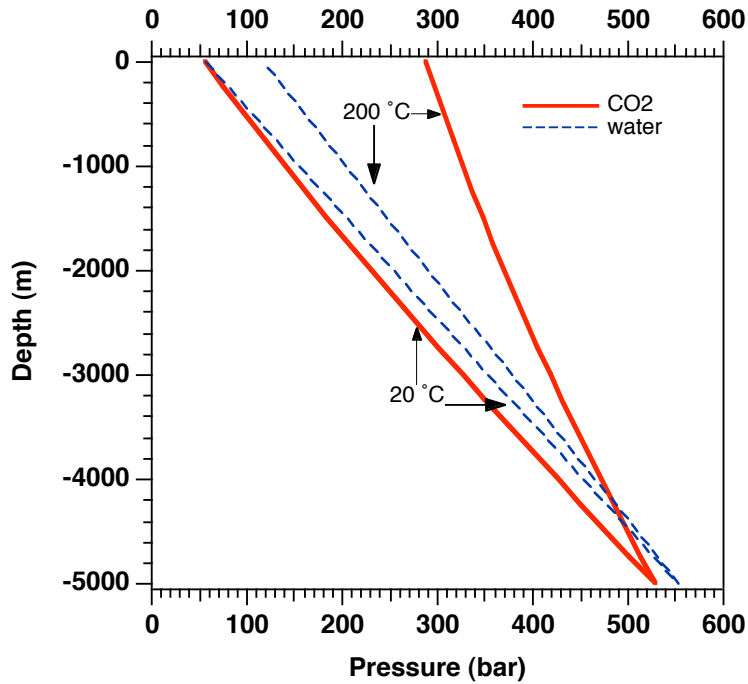
Figure 4. Static pressure profiles in CO_2 and water wells for constant temperatures of 20 and 200 ˚C, respectively.

We have calculated pressure and temperature conditions in static, isenthalpic columns of CO_2, using a similar recursion as for the constant-temperature wells considered above, except that now we need to consider temperature variation with depth as well, based on constant specific enthalpy. For an injection well, we perform a "top down" calculation starting from wellhead conditions of (T_0, P_0), corresponding to a specific enthalpy of $h_0 = h(T_0, P_0)$. At depth level n we have conditions of (T_n, P_n), from which we obtain $\rho_n = \rho(T_n, P_n)$ and $P_{n+1} = P_n + \rho_n g \Delta z$, just as before. The temperature at level n+1 is obtained as $T_{n+1} = T(P_{n+1}, h_0)$; the required inversion of the $h = h(T, P)$ relationship is accomplished by Newtonian iteration, using T_n as a starting guess. Fig. 5 shows (T, P)-profiles in a 5000 m deep injection well for several different wellhead temperatures and pressures. Fig. 6 shows (T, P)-profiles in a 5000 m deep production well for different downhole conditions.

Fig. 5 indicates that temperatures will tend to increase as CO_2 is flowing down the injection well and attaining increasing pressures. The difference between downhole and wellhead temperatures

is larger for smaller wellhead pressures, and increases strongly when wellhead temperatures are increased. For the lower wellhead temperature cases shown in Fig. 5, temperature changes versus depth are non-monotonic, with significant temperature decline at greater depth, especially when wellhead temperature is low and/or wellhead pressure is large.
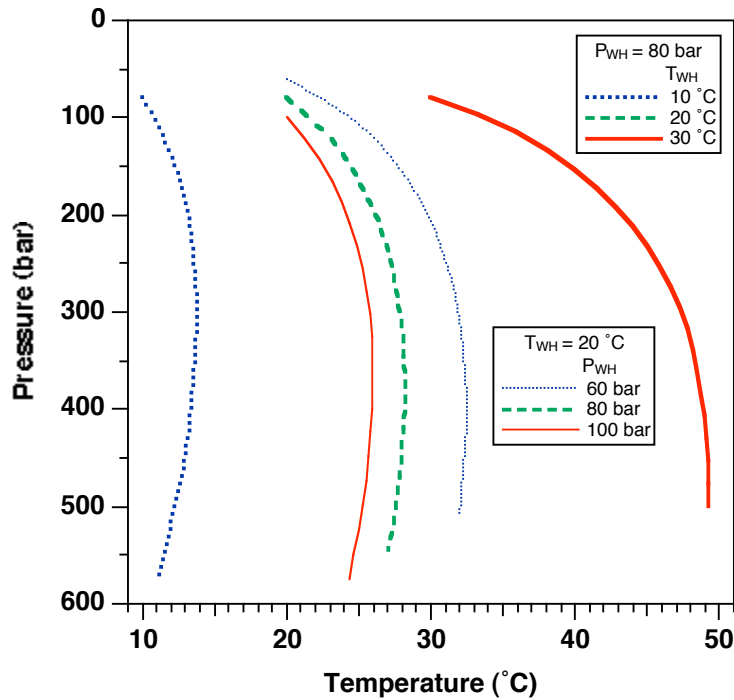

Figure 5. Temperature-pressure conditions for isenthalpic flow of CO_2 in a 5000 m deep injection well, for different wellhead temperatures and pressures.

These features can be understood from the dependence of specific enthalpy of CO_2 on temperature and pressure, see Fig. 3. For adiabatic (de-)compression processes, thermodynamic conditions will move along lines of constant enthalpy, indicating that compression starting from modest pressures and/or elevated temperatures will be accompanied by strong temperature increases. At temperatures below 50 °C, however, the isenthalps shown in Fig. 3 curve slightly backwards towards lower temperatures at high pressures, indicating that in this region isenthalpic compression will be accompanied by a temperature decline.
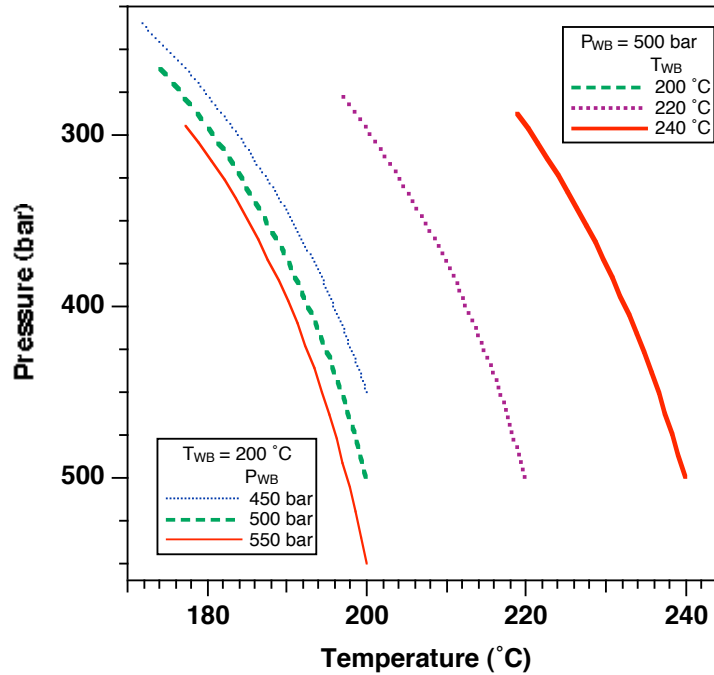
Figure 6. Temperature-pressure conditions for isenthalpic flow of CO_2 in a 5000 m deep production well, for different downhole temperatures and pressures.

Increased downhole temperatures in the injection well are favorable from the viewpoint of reservoir heat extraction, but they also reduce the pressure increase with depth in the injection well. This will reduce the buoyant pressure drive available for pushing CO_2 through the EGS reservoir, and will increase the power requirements for maintaining fluid circulation.

Analogous considerations apply to temperature and pressure behavior in production wells (Fig. 6). Here the isenthalpic decompression will cause CO_2 temperatures to decline as it flows up the well. The temperature drop along the well becomes stronger for smaller downhole pressures; at T_{WB} = 200 ˚C the temperature changes range from ΔT = -22.6 ˚C for P_{wb} = 550 bar to -25.7 ˚C at P_{wb} = 500 bar and -28.7 ˚C at P_{wb} = 450 bar. Temperature declines become smaller for increased downhole temperature. In the production well it is of course desirable to reduce temperature decline during fluid upflow as much as possible. This can be achieved by increasing downhole pressures, which however will require increased power consumption in the fluid circulation systems.

From this discussion it is apparent that optimal operation of a CO_2-EGS system will involve complex tradeoffs between reservoir heat extraction and power consumption in the fluid circulation system.

Fig. 7 presents static pressure profiles in CO_2 injection wells for 80 bar wellhead pressure and different wellhead temperatures. Downhole pressures decrease with increasing wellhead temperatures, and more so for adiabatic than for constant temperature conditions. This is because for adiabatic conditions wellbore temperatures are larger, and accordingly fluid densities are smaller. The differences in downhole pressures range from 5.3 to 33.3 bar (Table 2).

Table 2. Downhole pressures in CO_2 injection wells for 80 bar wellhead pressure and different wellhead temperatures, for isothermal and adiabatic conditions.

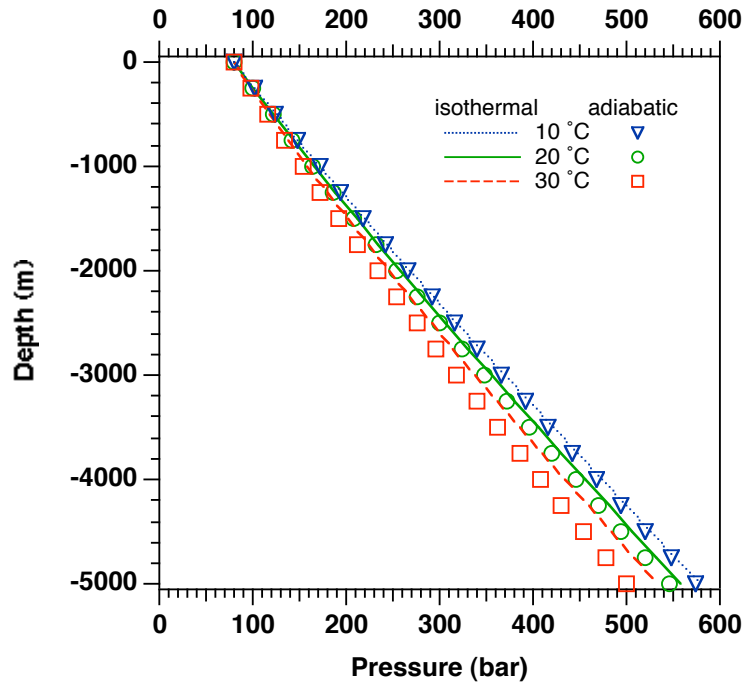| T (°C)	P_{ad} (bar)	P_{isoth} (bar)	ΔP (bar)
10	574.09	579.42	5.33
20	545.57	558.58	13.01
30	500.79	534.13	33.34

Figure 7. Static pressure profiles in CO_2 injection wells for 80 bar wellhead pressure and different wellhead temperatures. Profiles are shown for isothermal as well as adiabatic conditions.

RESERVOIR HEAT EXTRACTION

FIVE-SPOT FRACTURED RESERVOIR PROBLEM

In order to compare CO_2 and water as heat transmission fluids, we consider an idealized fractured reservoir problem whose parameters were loosely patterned after conditions at the European EGS site at Soultz (see Table 3; Baria et al., 2005; Dezayes et al., 2005). Instead of an injector-producer doublet, we consider a five-spot well configuration with a basic pattern area of 1 km^2 (production-injection well distance of 707.1 m; Fig. 8). This geometry is often chosen for fundamental studies of reservoir behavior, because the high degree of symmetry makes it possible to limit the model domain, which greatly simplifies the modeling problem (Sanyal and Butler, 2005). As seen in Fig. 8, the computational grid needs to cover only 1/8 of the domain,
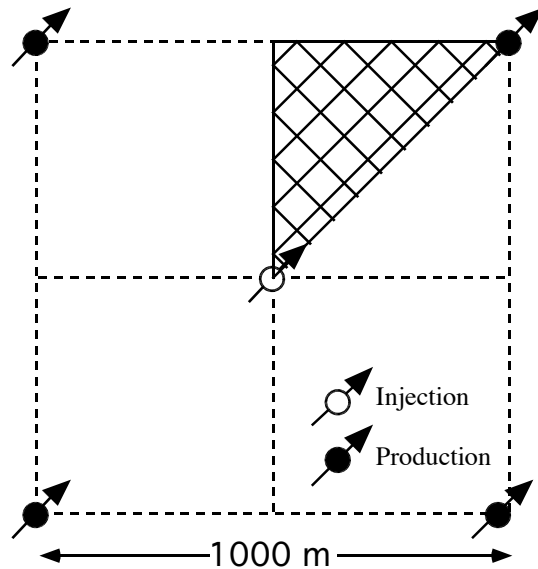
Figure 8. Five-spot well pattern with computational grid for modeling a 1/8 symmetry domain.

Table 3. Parameters for five-spot fractured reservoir problem.

Formation	
thickness	305 m
fracture spacing	50 m
permeable volume fraction	2%
permeability	50.0×10^{-15} m^2
porosity in permeable domain*	50%
rock grain density	2650 kg/m^3
rock specific heat	1000 J/kg/°C
rock thermal conductivity	2.1 W/m/°C
Initial Conditions	
reservoir fluid	all CO_2, or all water
temperature	200 °C
pressure	500 bar
Production/Injection	
pattern area	1 km^2
injector-producer distance	707.1 m
injection temperature	20 °C
injection pressure (downhole)	510 bar
production pressure (downhole)	490 bar

* we include some wall rock in the definition of the fracture domain

but results will be given on a "full well" basis. We use a two-dimensional 5-point grid of 36 square blocks with 70.71 m side length. Formation parameters, initial conditions, and production-injection specifications are given in Table 3.

We assume three orthogonal fracture sets with 50 m spacing, so that the matrix blocks enclosed by the fractures are cubes with (slightly less than) 50 m side length. The matrix blocks are assumed impermeable and are sub-gridded into 5 continua using the MINC approach (Pruess and Narasimhan, 1985). As colder injected fluid is migrating through the fracture system, it is heated by conduction from the matrix blocks. The problem is run in two variations, assuming the reservoir fluid to be either (liquid) water or supercritical CO_2. The simulations use our TOUGH2 code with a special fluid property module "EOSM" for mixtures of water and CO_2 (Pruess, 2004a, 2004b). Net heat extraction rates were calculated as $G_i = F_i h_i - (F_i h_i)_{inj}$ (i = CO_2, water), where F_i and h_i are mass flow rate and produced specific enthalpy, respectively, and $h_{i,inj}$ is injection enthalpy, evaluated at downhole conditions of (T, P) = (20 °C, 510 bar). Results for heat transfer rates and cumulative heat extraction are shown in Fig. 9.

For the system with CO_2 as heat transmission fluid, heat extraction rates are seen to be approximately 50 % larger than for water, which represents a very substantial acceleration of energy recovery. Fig. 10 shows a comparison of mass flow rates between the CO_2 and water cases. CO_2 mass flow rates are larger than those for water by a factor of approximately 3.7 initially, and decrease less over time than water flow rates. The initial factor of 3.7 seems surprisingly large, in view of the fact that the parameter group (ρ/μ) is only about a factor 1.9 larger for CO_2 than for water at initial reservoir conditions (see Fig. 2). However, for lower temperatures water viscosity increases much more than the viscosity of CO_2, giving CO_2 an additional advantage for flow in the vicinity of the injection well. Profiles of fluid pressures along a line from production to injection well show that for water much of the total pressure drop available for fluid circulation occurs in the cooled region near the injection well, while for CO_2 pressure gradients are only moderately stronger near the injection well than near the production well (Fig. 11).
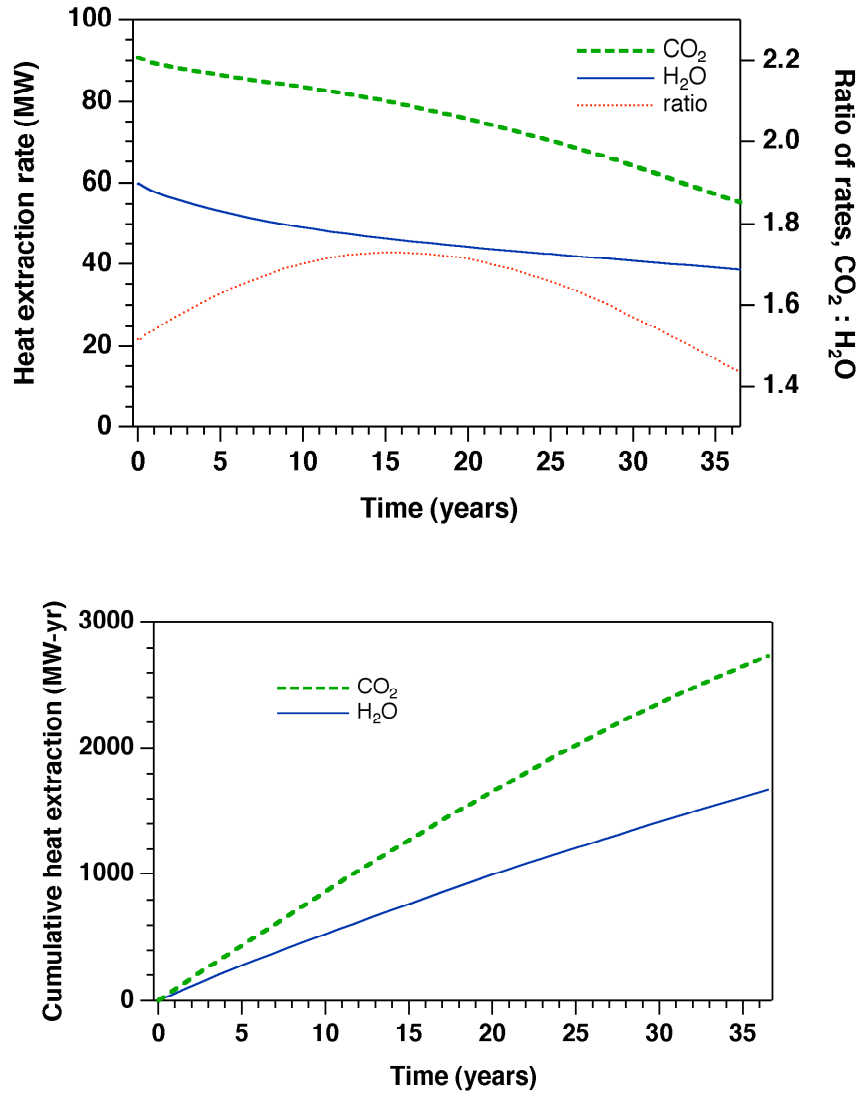
Fig. 9. Rate of net heat extraction (top) and cumulative heat produced (bottom) for the five-spot fractured reservoir problem (full well basis). The top frame also shows the ratio of heat extraction rates for the CO_2 and water systems.
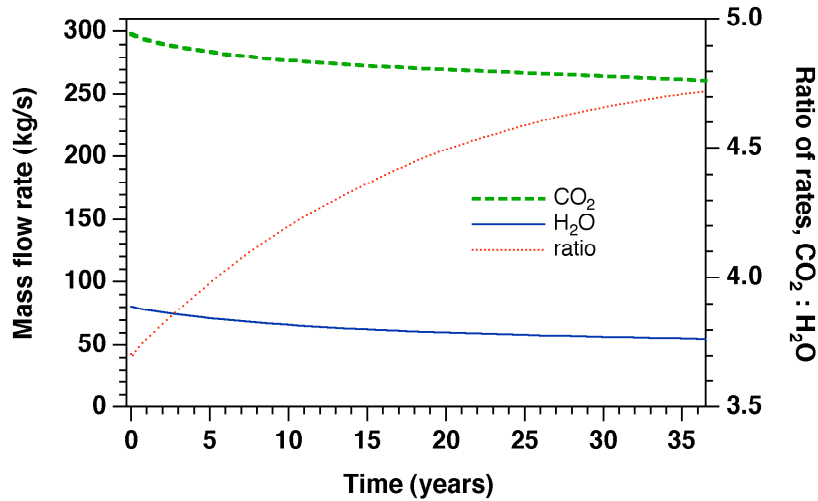
Figure 10. Mass flow rates for the five-spot problem. The ratio of flow rates in the CO_2 and water systems is also shown.
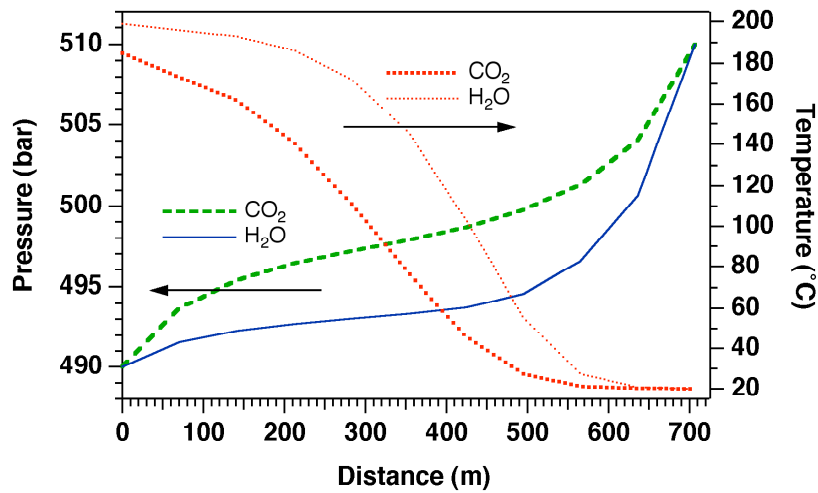

Figure 11. Pressure and temperature profiles along a line from production to injection well after a simulation time of 25 years.

SENSITIVITY STUDIES

Additional simulation studies were performed for reservoir parameters that were identical to the case considered above, except that different initial reservoir temperatures were used. Fig. 12 shows simulated ratios of net heat extraction rates for CO_2 and water for reservoir temperatures of 240, 200, 160, and 120 ˚C. (The 200 ˚C case is the one discussed above.) The comparison

shows that the acceleration of heat recovery when using CO_2 as compared to water is greater at lower temperatures. This suggests that serious consideration should be given to using CO_2 as heat extraction fluid not only for high-temperature resources that would be used for electricity generation, but also for lower temperature systems that would be produced for direct heat applications.

Fig. 13 compares the reference case with two alternatives, (1) injection temperature increased from 20 to 40 ˚C, and (2) reservoir pressure decreased from 500 to 400 bar. For higher injection temperature, the advantage of CO_2 as heat extraction fluid is reduced, while for lower reservoir pressure it is increased.
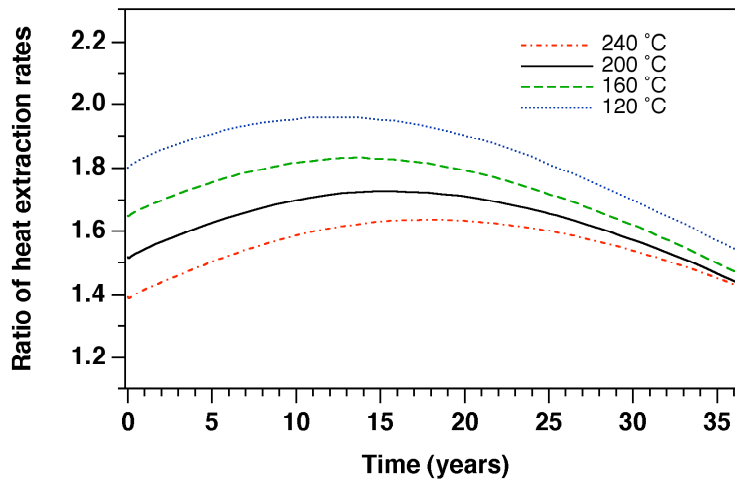

Figure 12. Ratios of net heat extraction rates (CO_2 vs. water) for different initial reservoir temperatures.
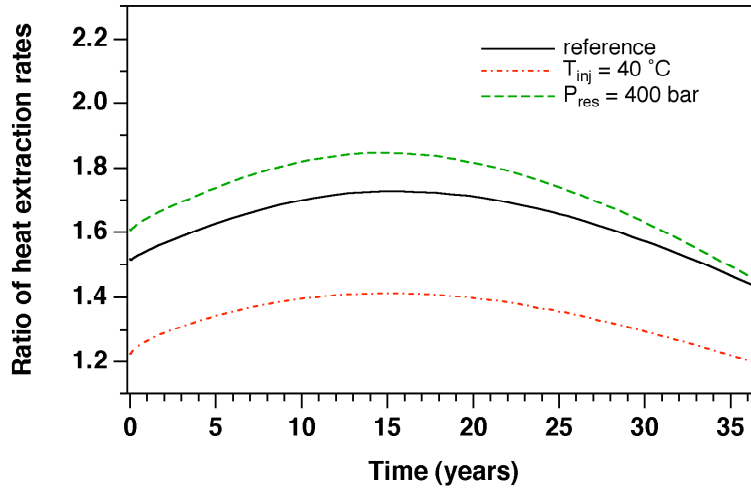
Figure 13. Ratios of net heat extraction rates (CO_2 vs. water) for different injection temperature and different reservoir pressure.

CO_2 STORAGE

Operating with CO_2 as heat extraction fluid, the reference case considered above generates approximately $Q = 75$ MW of thermal power, which for an assumed heat rejection temperature of 20 °C corresponds to a potential rate of mechanical work of $W = (1 - T_{rej}/T_{pro})*Q$. For $T_{rej} = 293.15$ K and $T_{pro} = 473.15$ K, the potential mechanical work is $W = 0.38Q = 28.5$ MW. Assuming a utilization efficiency of 0.45 (Sanyal and Butler, 2005), this translates into an electric power generation of $G = 0.45W = 12.83$ MW. The average mass production rate is approximately 280 kg/s, from which we deduce a fluid circulation requirement of approximately $280/12.83 = 21.8$ kg of CO_2 per MW electric power. No information is currently available on the fraction of CO_2 mass flow that would be lost in the reservoir due to different mechanisms; the loss rate likely depends on the site-specific permeability, porosity, water chemistry and mineralogy of the EGS reservoir. Long-term (almost one year) water circulation tests that were conducted at an experimental site at Fenton Hill, New Mexico, incurred water losses of 7-12 % of injected rates (Duchane, 1993). As fluid losses generally decrease over time, it appears reasonable for a first rough estimate to assume that long-term operation of a CO_2-based EGS would incur fluid losses on the order of 5 % of injected rate. From this figure, CO_2 losses can be estimated at approximately 1 kg/s per MW electric power, or 1 tonne per second per 1,000 MW.

To gain a perspective on this number, note that a large coal-fired power plant of 1,000 MW electric capacity generates approximately 30,000 tonnes of CO_2 per day (Hitchon, 1996). Our estimate then suggests that 1,000 MWe of installed CO_2-EGS could achieve geologic storage of the CO_2 generated by almost 3,000 MWe of coal-fired power generation. While these estimates are very rough and preliminary, they suggest that CO_2-EGS could provide a very large potential for geologic storage.

CHEMICAL ISSUES

A CO_2-based EGS is expected to comprise three zones (Fouillac et al., 2004; Ueda et al., 2005):

> Zone 1 - The inner zone or "core" of the system, from which all water has been removed by dissolution into the flowing CO_2 stream, so that the fluid consists of a single super-critical CO_2 phase. This is the main volume from which thermal energy is extracted by the flowing CO_2.

> Zone 2 - Surrounding the inner zone is an intermediate region that contains a two-phase mixture of CO_2 and aqueous fluid.

> Zone 3 - The outer region affected by the EGS activities. The fluid is a single aqueous phase with dissolved and chemically active CO_2.

Process behavior and issues are expected to be quite different in the different zones. This is especially true for chemical interactions. The outer reservoir zone would likely experience a combination of dissolution and precipitation effects that could impact reservoir growth and longevity. At the elevated temperatures of EGS, fluid-mineral reactions would be quite fast, providing a very favorable potential for rapid sequestration of CO_2 in the form of solid minerals (Fouillac et al., 2004; Ueda et al., 2005). The long-term behavior of the outer zone will be crucial for sustaining energy recovery, for estimating CO_2 loss rates, and for figuring tradeoffs between power generation and geologic storage of CO_2. The absence of water in the inner zone poses unique questions, as little is presently known about the geochemistry of non-aqueous systems. However, it seems clear that CO_2 would be a far less effective solvent than water. This would reduce the potential for dissolution and subsequent reprecipitation of minerals, and avoid

problems of scaling and formation plugging (Brown, 2000). It appears likely that prolonged exposure to supercritical CO_2 will cause dehydration reactions that would remove loosely bound water from rock minerals. Such reactions may reduce the molar volume of the minerals involved, which would increase porosity and permeability of the formations, and may promote reservoir growth (Pruess and Azaroual, 2006).

Aqueous solutions of CO_2 can be quite corrosive, and can dissolve different rock minerals, as well as attacking steel liners and casings used in well construction (Xu et al., 2005). However, aqueous fluids initially present in an EGS reservoir would be quickly removed by dissolution (evaporation) into the flowing CO_2 stream. Continuous operation of a CO_2-EGS would be expected to produce a rather dry CO_2 stream that would not pose corrosion problems for production wells.

CONCLUDING REMARKS

At typical temperature and pressure conditions anticipated for EGS - approximately 200 ˚C and a few hundred bars - CO_2 is a supercritical fluid with liquid-like density and gas-like viscosity. Its thermophysical properties make it quite attractive as a heat transmission fluid. Our exploratory studies suggest that CO_2 is superior to water in its ability to mine heat from an EGS reservoir. CO_2 appears to offer advantages for wellbore hydraulics as well, which may lead to reduced power consumption for maintaining fluid circulation. The geochemistry of supercritical CO_2, as opposed to aqueous solutions of CO_2, is not well characterized, and needs to be understood so that long-term behavior of reservoir porosity and permeability may be predicted.

Specific results of our modeling studies can be summarized as follows.
- Due to much larger expansivity and compressibility as compared to water, supercritical CO_2 will generate much stronger buoyancy forces between injection and production wells. This will reduce power consumption for the fluid circulation system, and may possibly allow adequate fluid circulation without external pumping.
- The compression of CO_2 flowing down an injection well and the expansion flowing up a production well will give rise to substantial temperature changes of as much as 10–25 ˚C.

Specifically, CO_2 will heat upon compression and cool upon expansion. These effects are in addition to temperature changes due to heat exchange between the wellbore and its surroundings and will tend to reduce the buoyant drive.

- For a given total pressure drop between injection and production wells, CO_2 will generate on the order of 4 times larger mass flows and 50 % larger net heat extraction rates as compared to water.

- The advantages of CO_2 in terms of accelerated energy extraction become larger for lower reservoir temperatures and pressures. CO_2 may be an attractive heat transmission fluid not only for high-temperature resources that would be used for electricity generation, but may offer even greater advantages for direct heat applications of lower-temperature resources.

- Based on fluid losses observed during long-term flow tests of the Fenton Hill hot dry rock system, fluid losses for CO_2-driven EGS are estimated as on the order of 1 tonne per second per 1,000 MW electric capacity. This means that 1,000 MWe of EGS-CO_2 could store all the CO_2 generated by 3,000 MWe of coal-fired power plants.

Fluid losses are an unavoidable aspect of engineered geothermal systems. Whereas the loss of water in a "conventional" EGS operation would be unfavorable and costly, fluid loss in an EGS system running with CO_2 would offer geologic storage of CO_2. Such storage may provide economic benefits and incentives in future carbon management scenarios where atmospheric emissions of CO_2 would be taxed, and avoidance of emissions could provide an additional revenue stream that would improve the economics of EGS.

REFERENCES

Altunin, V.V., *Thermophysical Properties of Carbon Dioxide,* Publishing House of Standards, 551 pp., Moscow, 1975 (in Russian).

Baria, R., S. Michelet, J. Baumgärtner, B. Dyer, J. Nicholls, T. Hettkamp, D. Teza, N. Soma, H. Asanuma, J. Garnish and T. Megel. Creation and Mapping of 5000 m deep HDR/HFR Reservoir to Produce Electricity, *Proceedings, Paper 1627.pdf,* World Geothermal Congress 2005, Antalya, Turkey, 24-29 April 2005.

Brill, J.P. and H. Mukherjee. *Multiphase Flow in Wells,* SPE Monograph, Vol. 17, Society of Petroleum Engineers, Richardson, TX, 1999.

Brown, D. A Hot Dry Rock Geothermal Energy Concept Utilizing Supercritical CO2 Instead of Water, *Proceedings,* Twenty-Fifth Workshop on Geothermal Reservoir Engineering, pp. 233–238, Stanford University, January 2000.

Dezayes, C., A. Genter and G.R. Hooijkaas. Deep-Seated Geology and Fracture System of the EGS Soultz Reservoir (France) based on Recent 5km Depth Boreholes, *Proceedings, Paper 1612.pdf,* World Geothermal Congress 2005, Antalya, Turkey, 24-29 April 2005.

Duchane, D. Hot Dry Rock Flow Testing – What has it Told us? What Questions Remain? *Transactions,* Geothermal Resources Council, Vol. 17, pp. 325–330, 1993.

Fouillac, C., B. Sanjuan, S. Gentier and I. Czernichowski-Lauriol. Could Sequestration of CO2 be Combined with the Development of Enhanced Geothermal Systems?, paper presented at Third Annual Conference on Carbon Capture and Sequestration, Alexandria, VA, May 3-6, 2004.

García, J.E., *Fluid Dynamics of Carbon Dioxide Disposal Into Saline Aquifers,* PhD dissertation, U. of California at Berkeley, Berkeley, California, December 2003.

Hitchon, B. (ed.). *Aquifer Disposal of Carbon Dioxide,* Geoscience Publishing, Ltd., Sherwood Park, Alberta, Canada, 1996.

IFC (International Formulation Committee). *A Formulation of the Thermodynamic Properties of Ordinary Water Substance,* IFC Secretariat, Düsseldorf, Germany, 1967.

Katz, D L. and R.L. Lee. *Natural Gas Engineering,* McGraw-Hill, New York, 1990.

Pruess, K. The TOUGH Codes—A Family of Simulation Tools for Multiphase Flow and Transport Processes in Permeable Media, *Vadose Zone J.,* Vol. 3, pp. 738 - 746, 2004a.

Pruess, K. Numerical Simulation of CO_2 Leakage from a Geologic Disposal Reservoir, Including Transitions from Super- to Sub-Critical Conditions, and Boiling of Liquid CO_2, *Soc. Pet. Eng. J.,* pp. 237 - 248, June 2004b.

Pruess, K. and M. Azaroual. On the Feasibility of Using Supercritical CO2 as Heat Transmission Fluid in an Engineered Hot Dry Rock Geothermal System, *Proceedings, Thirty-First Workshop on Geothermal Reservoir Engineering,* Stanford University, Stanford, CA, January 30 - February 1, 2006.

Pruess, K. and J.E. García, Multiphase Flow Dynamics during CO_2 Injection into Saline Aquifers, *Environmental Geology,* Vol. 42, pp. 282–295, 2002.

Pruess, K. and T.N. Narasimhan. A Practical Method for Modeling Fluid and Heat Flow in Fractured Porous Media, *Soc. Pet. Eng. J.,* 25 (1), 14-26, February 1985.

Ramey, H.J., Jr. Wellbore Heat Transmission, *J. Petrol. Tech.,* April 1962, pp. 427-435; *Trans., AIME,* Vol. 225, 1962.

Sanyal, S.K. and S.J. Butler. An Analysis of Power Generation Prospects from Enhanced Geothermal Systems, *Proceedings, Paper 1632.pdf,* World Geothermal Congress 2005, Antalya, Turkey, 24-29 April 2005.

Span, R. and W. Wagner. A New Equation of State for Carbon Dioxide Covering the Fluid Region from the Triple-Point Temperature to 1100 K at Pressures up to 800 MPa, *J. Phys. Chem. Ref. Data,* Vol. 25, No. 6, pp. 1509 - 1596, 1996.

Ueda, A., K. Kato, T. Ohsumi, T. Yajima, H. Ito, H. Kaieda, R. Meycalf and H. Takase. Experimental Studies of CO2-Rock Interaction at Elevated Temperatures under Hydrothermal Conditions, *Geochemical Journal,* Vol. 39, No. 5, pp. 417–425, 2005.

Vargaftik, N.B. *Tables on the Thermophysical Properties of Liquids and Gases*, 2nd Ed., John Wiley & Sons, New York, NY, 1975.

Xu, T. and K. Pruess. Numerical Simulation of Injectivity Effects of Mineral Scaling and Clay Swelling in a Fractured Geothermal Reservoir, *Transactions,* Geothermal Resources Council, Vol. 28, pp. 269–276, 2004.

Xu, T., J.A. Apps and K. Pruess. Mineral Sequestration of Carbon Dioxide in a Sandstone-Shale System, *Chemical Geology,* Vol. 217, pp. 295–318, 2005.